Magnetic-field asymmetry of electron wave packet transmission in bent channels capacitively coupled to a metal gate

R. Kalina,[1] B. Szafran,[1] S. Bednarek,[1] and F.M. Peeters[2]

[1]*Faculty of Physics and Applied Computer Science,*
AGH University of Science and Technology, al. Mickiewicza 30, 30-059 Kraków, Poland
[2]*Departement Fysica, Universiteit Antwerpen, Groenenborgerlaan 171, B-2020 Antwerpen, Belgium*

We study the electron wave packet moving through a bent channel. We demonstrate that the packet transmission probability becomes an uneven function of the magnetic field when the electron packet is capacitively coupled to a metal plate. The coupling occurs through a non-linear potential which translates a different kinetics of the transport for opposite magnetic field orientations into a different potential felt by the scattered electron.

The current (I) that flows through mesoscopic conductors in contact with electron reservoirs is expressed as the product of the voltage (V) applied to the leads and the conductance (G) which in the linear transport regime depends on the external magnetic field (B) but not on the voltage, $I(B,V) = G(B)V$. According to the Landauer theory the linear conductance (G) of a two-terminal conductor $G(B) = \frac{e^2}{h}T_{12}(B)$, is proportional to the transfer probability of a Fermi level electron from terminal 1 to terminal 2 (T_{12}). For a conductor with disorder (or in general with a potential landscape) that is independent of B, or is an even function of B, the transmission probability is symmetric with respect to the magnetic field orientation. The relation

$$T_{12}(B) = T_{12}(-B), \qquad (1)$$

known as Onsager symmetry when expressed in terms of conductance, can be derived in the scattering matrix theory [2]. Time-reversal symmetry alone gives only $T_{12}(B) = T_{21}(-B)$, which is due to the fact that the electron trajectory from terminal 1 to 2 deflected by the Lorentz force for magnetic field $+B$ coincides with the trajectory from 2 to 1 and opposite field orientation $-B$. The symmetry (1) results from the backscattering probability being an even function of the magnetic field $R_{11}(B) = R_{11}(-B)$, since the backscattered trajectories are independent of the magnetic field orientation [see Fig. 1(a)]. Recently it was pointed out [3] that a current asymmetry $I(B,V) \neq I(-B,V)$ can occur in the non-linear transport regime, i.e., when the conductor is driven out of equilibrium. Magnetic-field asymmetry of the non-linear conductance was indeed found in carbon nanotubes [4], quantum billiards [5] rings [6] and dots [7].

In this Letter we report on simulations of the transport of an electron packet through a bent semiconductor channel that is capacitively coupled to a metal plate. In gated semiconductor nanodevices [8] the confined charge carriers are capacitively coupled to the electrodes. The coupling is described by the Schrödinger-Poisson scheme [9]. The electron wave packet induces a redistribution
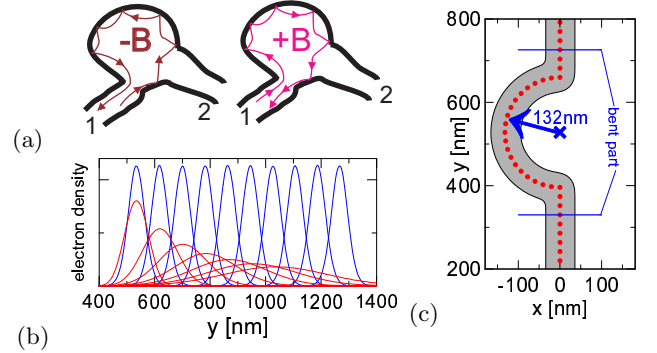

FIG. 1: (color online) (a) Backscattered trajectories for opposite magnetic field orientations. For $-B$ ($+B$) the trajectories are deflected to the right (left) by the Lorentz force. (b) Snapshots of the wave packet density along the axis of the straight wire that is covered (blue lines) and uncovered (red lines) by a metal plate. c) Dots show the position of the centers of the basis function [Eq. (2)] defining the channel. Shaded area shows the channel range determined as the region where the sum of the absolute values of the basis functions is larger than 6.5% of its maximum value. The horizontal lines show the range of the bent part $y \in [330\text{nm}, 726\text{nm}]$.

of the charge on the surface of the metal. The redistributed charge on the metal surface is a source of potential that focuses the electron wave function and stabilizes the shape of the packet when it is set in motion [10]. The electron density interaction with the metal is non-linear and results in a cancelation of dispersion effects intrinsically present in the linear Schrödinger equation [11]. For that reason the electron wave packet interacting with the metal has a soliton character. We demonstrate below that the transmission probability of the electron soliton through a bent channel is an uneven function of the magnetic field.

Our simulation is based on a numerical solution of the two-dimensional time-dependent Schrödinger equation $i\hbar\frac{\partial\Psi}{\partial t} = H\Psi$. We use an approach [12] originally introduced to describe the attenuation of the Aharonov-Bohm oscillations by the preferential injection of the in-

coming wave packet to one of the arms of the quantum ring by the Lorentz force. The kinetic energy Hamiltonian is given by $T = (-i\hbar\nabla + e\mathbf{A})^2/2m^*$. The Landau gauge $\mathbf{A} = (-By, 0, 0)$, GaAs electron effective mass $m^* = 0.067m_0$ and dielectric constant $\epsilon = 12.4$ are used. The time evolution is calculated in the basis of Gaussian functions $\Psi(\mathbf{r}, t) = \sum_n c_n(t)f_n(\mathbf{r})$, where

$$f_n(\mathbf{r}) = \exp\{-\alpha(\mathbf{r} - \mathbf{R}_n)^2 + i\beta(x - X_n)(y + Y_n)\}, \quad (2)$$

with $\mathbf{r} = (x, y)$, $\beta = eB/2\hbar$, $\alpha = 1/(22\text{nm})^2$ and $\mathbf{R}_n = (X_n, Y_n)$ is the center of the n-th Gaussian. The imaginary term in (2) is related to the magnetic translation and ensures gauge invariance. In the applied approach the centers $\mathbf{R}_n$ define the structure itself. The choice modeling the bent channel is shown in Fig. 1(c).

We assume that at a distance $d = 20$ nm above the channel the structure is covered by an infinite metal plane. For infinite plane the solution of the Poisson equation [10] for the response of the metal can be obtained with the image-charge technique [11]. Interaction energy of the electron density with metal introduces is therefore given by

$$V(\mathbf{r}, t) = \int \frac{-|e\Psi(\mathbf{r}', t)|^2 d\mathbf{r}'}{4\pi\epsilon\epsilon_0 \left[(x - x')^2 + (y - y')^2 + (2d)^2\right]^{1/2}}. \quad (3)$$

All the time dependence of the wave function (2) is introduced in the expansion coefficients $c_n(t)$. Equations for $c_n(t)$ are obtained from the Crank-Nicolson differential scheme $i\hbar\left[\Psi(t + \Delta t) - \Psi(t)\right]/\Delta t = \left[H(t + \Delta t)\Psi(t + \Delta t) + H(t)\Psi(t)\right]/2$. The Hamiltonian depends on time through the induced potential $H(t) = T + V(t)$. For the basis (2) the Crank-Nicolson scheme is given by a system of equations $\mathbf{S}\mathbf{c}(t + \Delta t) = \mathbf{S}\mathbf{c}(t) - \frac{i\Delta t}{2\hbar}\left[\mathbf{H}(t + \Delta t)\mathbf{c}(t + \Delta t) + \mathbf{H}(t)\mathbf{c}(t)\right]$, where the overlap and Hamiltonian matrix elements are given by $\mathbf{S}_{mn} = \langle f_m|f_n\rangle$ and $\mathbf{H}_{mn}(t) = \langle f_m|H(t)|f_n\rangle$, respectively. As the initial condition we take a self-focused wave packet [11] localized 500 nm before the bent segment moving [12] along the incoming wire with average kinetic energy $\hbar^2 k^2/2m^* = 1.4$ meV ($k = 0.05$/nm).

A comparison of the motion of the soliton and normal (i.e. non-interacting with metal) wave packet moving in a straight channel is shown in Fig. 1(b). Scattering on the bent segment is illustrated in Fig. 2 which shows the density of the moving packet at specific times (increasing from top to bottom figures) for the situation without (two left columns) and with a metal gate present (two right columns) for $B = \pm0.75$T. For positive value of the field the wave packet is deflected to the left by the Lorentz force as it moves up [see also Fig. 1(b)] and thus it is injected into the bent of the wire [Figs. 2(a,e)]. For negative B value the injection occurs only after the velocity of the packet is inverted [Fig. 2(e,m)] when the packet is reflected at the entrance. This introduces a delay in the transport of the packet for negative B value.
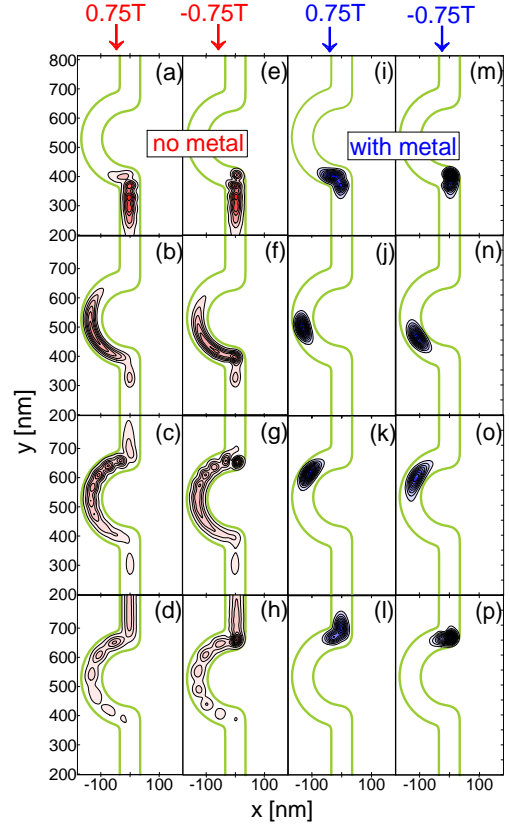

FIG. 2: (color online) Snapshots of the motion of the electron packet injected into the bent wire from the lower lead for opposite magnetic field orientations. Later moments in time correspond to lower plots. Solution of the linear Schrödinger equation (a-h) is presented for $t = 2.1, 4.8, 6.7$ and 9.5 ps and the solution including the non-linear term of the wave packet-metal interaction (i-p) is given for $t = 3.4, 5.8, 7.7$ and 9.7 ps. Green lines delimit the channel as defined in Fig. 1(c).

More details of the motion are seen on the plots of the density taken along the straight part of the wires ($x = 0$). For $B = -0.75$ T we notice [Fig. 3(a)] a compression of the wave packet which occurs when the packet is reflected at the entrance and at the exit of the bent part. No compression is seen for $B = 0.75$ T, for which the Lorentz force guides the packet into the bent and out of it without reflection at the junctions. For both $B = \pm0.75$ T the wave packet transfer probability is nearly 95% and no reflected part of the packet can be noticed at this scale of the plot. The reflected part is visible for zero magnetic field [Fig. 3(b)]. In all cases the transmitted packet stays more or less compact, but with a shape that changes in time. The breathing of the transmitted wave packet is due to deviations of its form from the stable one that occurs during the transfer through the bent segment. For $B = +0.75$ T the breathing is nearly absent, and it is strongest for $B = -0.75$ T for which wave packet compression at the junctions occurs. The results for the normal packet are given in Fig. 4(a) where the
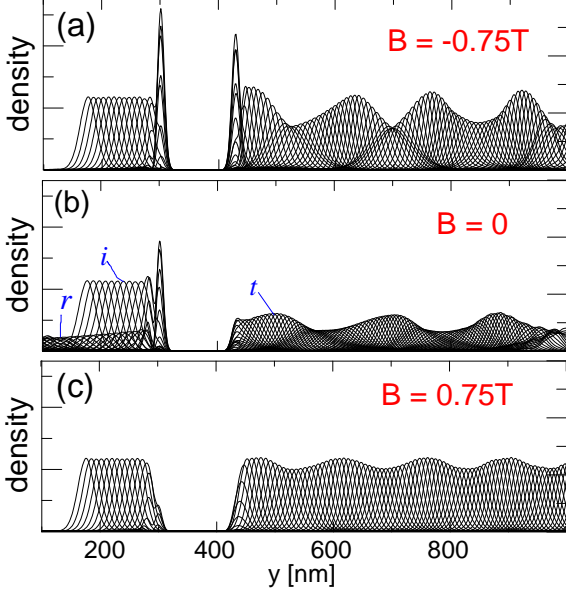
FIG. 3: (color online) The snapshots of the packet density along the axis of the straight channels ($x = 0$) for the electron interacting with metal for $B = -0.75$ T, 0 and 0.75 T in (a), (b) and (c), respectively. In (b) the incoming, reflected and transmitted wave packets are marked by i, r and t, respectively.
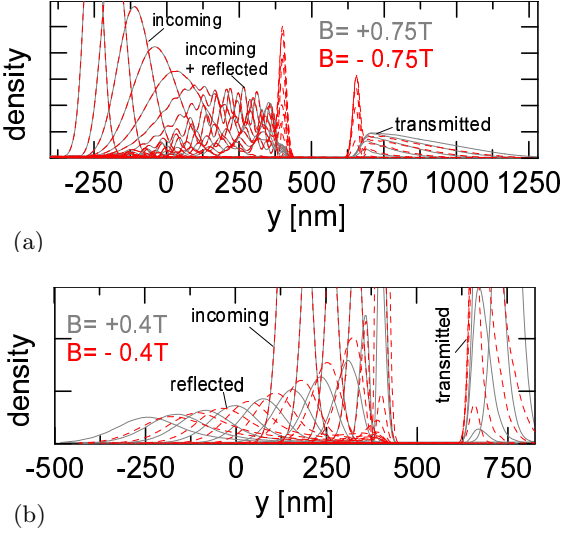

FIG. 4: (color online) Same as Fig. 3 for the normal wave packet (a) and a wave packet interacting with the metal plate (b).

densities are calculated at the same moments in time for both field orientations. Both densities in the straight wire are exactly the same in the region before the bent part for the incoming wave packet as well as for the interference which occurs when slower (still incoming) and faster (already reflected) parts of the wave packet meet below the bent. Note that such an interference was not

observed for the soliton wave packet. Differences in the shape of the packet for $B = \pm 0.75$ T are clearly visible at the entrance to the bent (compression for negative B) and in the transmitted wave packet. The reflected part of the soliton scattering for $B = \pm 0.4$ T is observed in Fig. 4(b). Only the plots for the incoming wave packet coincide for both B orientations. The snapshots of the reflected parts of the wave packet are no longer the same when the magnetic field is inverted. We observe here a destruction of the soliton which is split into two parts. Note, that the reflected part of the scattered soliton [see Fig. 4(b)] spreads like a normal wave packet. The image charge of this part is not large enough to focus it.

The time-dependence of the fraction of the wave packet inside the bent as well as in the straight wires before and after the bent [see Fig. 1(c)] are shown in Fig. 5(a) for the normal packet and in Fig. 5(b) for the soliton. In the absence of the metal the fraction of the wave packet before the bent is exactly the same for both ± 0.4 T. Since the bent segment does not permanently capture any part of the normal packet the fraction of the packet which is eventually transmitted to the outgoing wire is the same for both B orientations. For the wave packet interacting with the metal [see Fig. 5(c)] the reflected part of the wave packet before the bent segment is different for ± 0.4 T and a different transmission probability is obtained. Soliton destruction is inelastic and associated with decreased absolute value of both electron-metal interaction energy and the kinetic energy of the packet.

The fraction of the wave packet which is transmitted into the outgoing wire at the end of the simulation is a *lower bound* to the transmission probability. A small fraction of the wave packet still bounces back and forth within the bent leaving it in small portions to the incoming and to the outgoing wires. For that reason the sum of the transmitted wave packet and the part which is still present in the bent at the end of the simulation is an *upper bound* to the transmission probability. The bounds on $T(B)$ for the wave packet interacting with the metal plate are plotted in Fig. 5(c). We conclude that the transmission probability is: i) an uneven function of the magnetic field, and ii) for $B > 0.1$ T the asymmetry in the transmission probability for opposite B orientations exceeds the evaluation accuracy.

In the absence of the metal plate the fraction of the normal packet in the incoming lead $R(B, t)$ is an even function of the magnetic field at any moment in time. In general also for the normal packet the transferred fraction is different for opposite field orientations, i.e. $T(B, t) \neq T(-B, t)$, and a symmetric transfer probability is obtained only in the large t limit. The kinetics of the transfer of both normal and solitary packets through an asymmetric channel is different for opposite field orientations. The different kinetics for the wave packet interacting with the metal is translated into a different potential felt by the scattered electron. For that reason the ar-
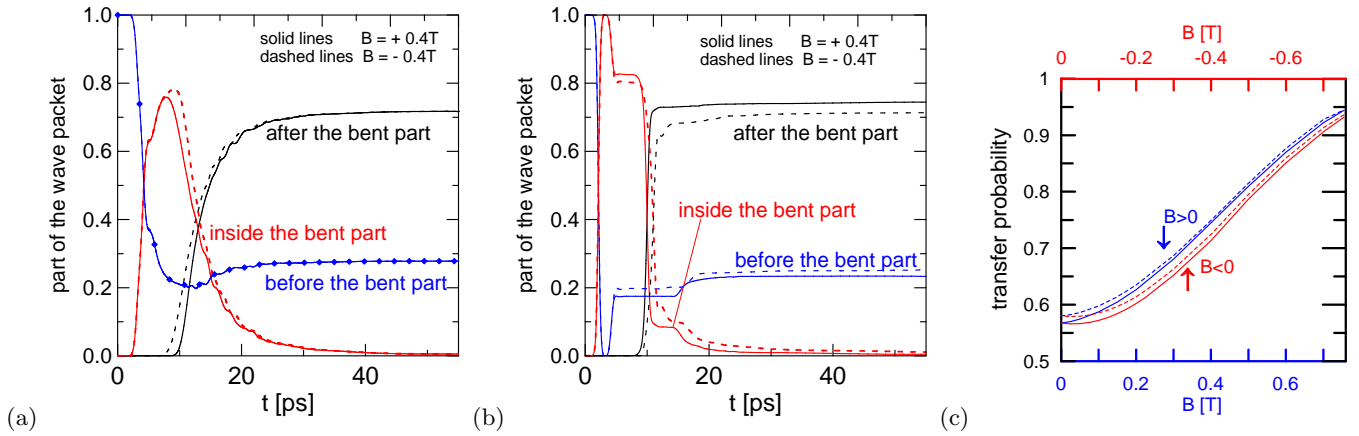
FIG. 5: (color online) Parts of the wave packet before, after and inside the bent part of the wire for the electron density uncoupled (a) and coupled (b) to the metal plate. Solid lines show the results for $B > 0$ and dashed lines for $B < 0$. In (a) the part 'before' the packet for $B < 0$ is given by the symbols. (c) Lower (solid) and upper (dashed) curves are bounds for the wave packet transfer probability for $B > 0$ (blue lines) and $B < 0$ (red lines).

gument of the equivalent backscattered trajectories for opposite B orientations [cf. Fig. 1(a)] does not hold in the present case. The effective scattering potential is different when the magnetic field is inverted and consequently $R(B,t) \neq R(-B,t)$, also in the large t limit. The reason of the magnetic-asymmetry is the asymmetry of the inelastic soliton destruction for $\pm B$.

To further convince ourselves, we studied the case of the electron dynamics governed by the Gross-Pitaevski equation [13] in which the potential (3) is replaced by $V(\mathbf{r},t) = -\gamma|\Psi(\mathbf{r},t)|^2$ with $\gamma > 0$ (obtained for $1/r_{12}$ replaced by Dirac $\delta(r_{12})$ in the integrand of (3)). For this potential the Hamiltonian matrix elements can be evaluated analytically. We found that also in this case the transmission probability is asymmetric in B.

The presented theory was applied to an empty ballistic channel that is capacitively coupled to a metal plate with a carefully prepared initial wave packet. The channel is not connected to electron reservoirs and thus the modeling does not correspond to an electron gas in equilibrium. Although the theory does not allow us to calculate the current, it is nevertheless related to the previous work on the magnetic-field asymmetry of non-linear conductance. In the original idea [3] it was the dependence of the potential landscape on B that resulted in the asymmetry. In our model the role of the landscape is played by the response potential of the metal which depends on B orientation through the time dependence of the image charge. In previous work [14] it was pointed out that the uneven modification of the potential landscape and the resulting magneto-asymmetry of non-linear transport is due to the Coulomb interaction. In our case the moving electron wave packet interacts with the electrons in metal. It was recently explained that the Onsager symmetry is broken for conductors interacting with the environment [15]. A second conductor [15] was used as the

environment which was driven out of equilibrium by the applied bias. In the present work the metal is perturbed by the moving wave packet.

In conclusion, we demonstrated that the transfer probability of an electron wave packet through a semi-circular channel in interaction with a metal plate, that leads to a non-linear potential, is not an even function of the magnetic field.

[1] M. Büttiker, Phys. Rev. Lett. **57**, 17612 (1986).

[2] C.W.J. Beenaker, Rev. Mod. Phys **69**, 731 (1997).

[3] D. Sánchez and M. Büttiker, Phys. Rev. Lett. **93**, 106802 (2004).

[4] J. Wei *et al.*, Phys. Rev. Lett. **95**, 256601 (2005).

[5] C.A. Marlow *et al.*, Phys. Rev. Lett. **96**, 116801 (2006).

[6] R. Leturcq *et al.*, Phys. Rev. Lett. **96**, 126801 (2006).

[7] D.M. Zumbühl *et al.*, Phys. Rev. Lett. **96**, 206802 (2006).

[8] R. Hanson *et al.* Phys. Rev. Lett. **94**, 196802 (2005); J.M. Elzerman *et al.* Nature **430**, 431 (2004).

[9] D.V. Melnikov *et al.*, Phys. Rev. B **72**, 085331 (2005); M. Stopa, Phys. Rev. B **63**, 195312 (2001); **54**, 13767 (1996); S. Bednarek *et al.* Phys. Rev. B **64**, 195303 (2001); **68**, 155333 (2003); **77**, 115320 (2008).

[10] S. Bednarek *et al.* Phys. Rev. Lett. **100**, 126805 (2008).

[11] S. Bednarek, B. Szafran, and K. Lis, Phys. Rev. B **72**, 075319 (2005); **73**, 155318 (2006).

[12] B. Szafran and F.M. Peeters, Phys. Rev. B **72**, 165301 (2005).

[13] K. Bongs *et al.*, Phys. Rev. Lett. **83**, 3577 (1999).

[14] M. Büttiker and D. Sánchez, Int. J. Quantum Chem. **109**, 906 (2005); E. Deyo, B. Spivak, and A. Zyuzin, Phys. Rev. B **74**, 104205 (2006).

[15] D. Sánchez and K. Kong, Phys. Rev. Lett. **100**, 036806 (2008).